Cement and Concrete Research 40 (2010) 598–604

Contents lists available at ScienceDirect

Cement and Concrete Research

journal homepage: http://ees.elsevier.com/CEMCON/default.asp

Influence of steel fibers on the development of alkali-aggregate reaction

Maria Rita Pires de Carvalho [a], Eduardo de Moraes Rego Fairbairn [a,*], Romildo Dias Toledo Filho [a], Guilherme Chagas Cordeiro [b], Nicole Pagan Hasparyk [c]

[a] COPPE/Universidade Federal do Rio de Janeiro, Civil Engineering Department, P.B. 68506, CEP 21941-972, Rio de Janeiro-RJ, Brazil
[b] Universidade Estadual Norte Fluminense Darcy Ribeiro, Laboratory of Civil Engineering, Campos dos Goytacazes-RJ, Brazil
[c] FURNAS Centrais Elétricas S.A., DCT.C., Aparecida de Goiânia-GO, Brazil

ARTICLE INFO

Article history:
Received 26 February 2009
Accepted 17 November 2009

Keywords:
Alkali-aggregate reaction (C)
Fiber reinforcement (E)
Mortar (E)
AAR accelerated test

ABSTRACT

This work presents the results of an experimental research concerning the use of fibers in mortar specimens subjected to alkali-aggregate reaction (AAR). Two types of steel fibers (0.16 mm diameter and 6.0 mm length, and 0.20 mm diameter and 13.0 mm length) were used with fiber volume contents of 1% and 2%. Besides the expansion accelerated tests, compressive tests and flexural tests have also been carried out to display the main mechanical characteristics of the fiber-reinforced mortars after being subjected to AAR. Moreover, the microstructure of the specimens was analyzed by scanning electron microscopy and energy dispersive X-ray. The results shown that the addition of steel fibers reduced the expansion due to AAR for the experimental conditions studied in this paper. The most expressive benefit corresponded to the addition of 13.0 mm fibers in the mixture containing 2% fiber content. This fiber volume content also corresponded to the maximum increment in the mechanical properties compared to the reference mortar, mainly for the post-cracking strength and for the toughness in bending. It was observed that the fibers have a beneficial effect on the material, without compromising its main mechanical properties.

1. Introduction

In a recent research and development joint project (R&D), the Brazilian hydropower industry — FURNAS Centrais Elétricas S.A. and the Federal University of Rio de Janeiro have studied the use of fibers to replace reinforcement bars in structural members used in hydroelectric power plants [1]. This could accelerate the construction of the plant, as time and material are economized. Since the hydropower plants are prone to the development of alkali-aggregate reaction (AAR), it is worthwhile to study the behavior of the fiber-reinforced material when subjected to this deleterious reaction.

There are few references concerning the influence of fibers on the development of AAR in the specialized literature. Turanli et al. [2] analyzed the use of steel microfibers in fiber volume contents ranging from 1% to 7%. The authors observed that the use of fibers significantly reduced the expansion and cracking due to AAR. However, for the volume of 1% the beneficial effect depended on the curing time. The authors also proposed that the microfibers are more efficient than conventional fibers because their small length allows a placement close to the interface of the reactive aggregates, thus influencing the early gel formation. To proof the hypothesis of Turanli et al. [2], Garci et al. [3] developed a special type of aggregate with embedded microfibers (fiber volume of 0.5%) and observed that the expansion reduced by 25%. More recently, Ostertag et al. [4] used a mixture with fiber volume of 7% of steel microfibers and observed that the beneficial effect of steel fibers comes from the mechanical confinement of the gel produced by the reaction. Haddad and Smadi [5] evaluated the role of steel fibers (fiber volume contents of 0.5% and 1.0%) and polypropylene (0.15%). They concluded that, for these fiber volumes, the fibers contributed moderately to reduce the expansion due to AAR. However, the extent of cracking was found to be limited by the use of fibers. Park and Lee [6] analyzed the efficiency of steel fibers in mortars containing aggregates of waste glass. They observed that the addition of 1.5% of fibers to concrete containing 20% waste glass can reduce the expansion ratio up to 40% and increase the flexural strength up to 110%.

In this work, the results of an experimental research on the use of steel fibers in mortars subjected to AAR are presented. Two types of steel fibers (0.16 mm diameter and 6.0 mm length, and 0.20 mm diameter and 13.0 mm length) were used with fiber volume contents of 1% and 2%. Besides the expansion tests performed in a procedure similar to ASTM C-1260, compressive and flexural tests, and microscopy analysis have also been carried out to display the main mechanical and microstructural characteristics of the fiber-reinforced material subjected to AAR.

It should be emphasized that, for economical reasons, the aggregates used for the construction of a dam are generally those available in the region close to the construction site or even those quarried from the

* Corresponding author. Tel.: +55 21 25628481.
E-mail address: eduardo@coc.ufrj.br (E.M.R. Fairbairn).

0008-8846/$ – see front matter © 2009 Elsevier Ltd. All rights reserved.
doi:10.1016/j.cemconres.2009.11.007

excavations. Although several measures are nowadays taken to prevent the AAR in modern concrete mix-design, a possible benefic effect of the fibers is not considered when the consequences of the reaction and its evolution are evaluated. This is because the phenomenon is not yet well understood and only few references have been dedicated to this subject. Hence, the present research aims to contribute with new experimental data concerning the influence of the fibers on the development of alkali-aggregate reaction.

2. Materials and methods

2.1. Materials

The cement used was a Portland cement CPI-32 (similar to ASTM type I) with high content of alkalis, without any admixture. The main characteristics of this cement are presented in Table 1. Diabasic rocks were used as reactive aggregate. Petrography analysis carried out in the Laboratory of FURNAS (Brazilian Hydropower Company), indicated gray massive igneous rock. Microscopic analysis indicated that it is composed by feldspar (50 to 55% in mass), pyroxene (35 to 40%), and opaque minerals (10%). It was also verified in the rock a fine grained matrix suggesting the presence of volcanic glass as indicator of its reactive potentiality. Its density is 3000 kg/m^3 and the grain size distribution, shown in Table 2, is in accordance with the requirements of ASTM C-1260 [7]. This rock was considered deleterious for ASR according to ASTM C-1260 test method.

Two types of steel fibers were used: (i) 0.16 mm diameter (D) and 6.0 mm length (L), having an aspect ratio (L/D) equal to 37.5; and (ii) 0.20 mm diameter and 13.0 mm length, having a L/D equal to 65. The density and nominal tensile strength of the fibers were equal to 7900 kg/m^3 and 2200 MPa, respectively.

2.2. Experimental methods

Five mortars with Portland cement and diabasic aggregate were produced, varying the steel fiber volume content in 0%, 1.0% and 2.0% for the two types of fibers. The five mixtures are denominated: 0%SF, 1%SF6, 2%SF6, 1%SF13 and 2%SF13, where the first number indicates the fiber volume content (0, 1 or 2%) and the last number denominates the fiber length (6 or 13 mm). The reference mixture is the 0%SF.

Table 1
Main physicochemical properties of the cement[a].

Density		3.12 g/cm^3
Residue on sieve 200		1.7
Residue on sieve 325		12.2
Specific surface area		311 m^2/kg
Compressive strength	3 days	20.4 MPa
	7 days	25.9 MPa
	28 days	31.3 MPa
Loss on ignition		1.55
Insoluble residue		0.35
SO_3		2.44
MgO		1.16
SiO_2		20.75
Fe_2O_3		2.56
Al_2O_3		4.52
CaO		64.65
Free lime		3.0
Total alkali	Na_2O	0.77
	K_2O	0.84
	Alkali equivalent[b]	1.32
Soluble alkali	Na_2O	0.34
	K_2O	0.75
	Alkali equivalent[b]	0.83
$CaSO_4$		4.15

[a] Units in % by mass where not specified.
[b] Na_2O eq. $= Na_2O + 0.658 \cdot K_2O$.

Table 2
Grain size distribution of aggregate.

Sieve	% by mass
4.8 mm to 2.4 mm	10
2.4 mm to 1.2 mm	25
1.2 mm to 0.6 mm	25
0.6 mm to 0.3 mm	25
0.3 mm to 0.15 mm	15

The experimental procedure was similar to ASTM C-1260 [7], with some adaptations to meet the specific conditions of the fiber-reinforced material. In this case, the dimensions of the three specimens were taken to be 75×75×285 mm (and not the conventional 25×25×285 mm). After curing for 28 days in a high-humidity chamber (21±1 °C; 100% RH) the specimens were immersed in a water bath and subjected to a temperature rising up to 60 °C. The specimens were kept in this bath for approximately 4 h until the thermal dilatation was considered as stabilized. Then, the specimens were transferred to another bath containing a sodium hydroxide 1 N solution at temperature 60±2 °C for 60 days. The length change measurements were taken with the specimen vertically fitted to a stainless-steel frame with one extremity fixed to a displacement gauge according to ASTM C- 490 [8].

The compressive strength, Young's modulus and four-point bending were carried out in the mechanical evaluation of the mortars. These tests were performed in the following ages: (i) 28 days (straight after being removed from the curing chamber); (ii) 42, 56 and 88 days (i.e., 14, 28 and 60 days after immersion in the NaOH 1 N solution, respectively). Compressive strengths were determined for 75 mm diameter and 150 mm height specimens. Young's modulus was calculated using the stress–strain curves according to ASTM C-469 [9]. Four-point bending tests were performed, following the standards Mercosur NM 55:96 [10], on prismatic specimens having the dimension 50×50×228 mm. The flexural toughness index has been calculated according to JCI-SF4 [11]. The mechanical tests were also performed in a 1000 kN Shimadzu testing machine at a displacement rate of 0.1 mm/min.

Although the samples used in this study present different sizes the authors decided to attend the recommendations of international standards regarding to the geometry generally used in the compression and bending tests once the main objective of the tests was to establish, in a comparative way, the influence of the fiber reinforcement in the stress–strain and load-deflection behavior of the material subjected to the NaOH environment.

Microscopic analysis was carried out with a scanning electron microscope (SEM) linked to energy dispersive X-ray (EDX) allowing the qualitative analysis of the chemical elements of AAR products. The

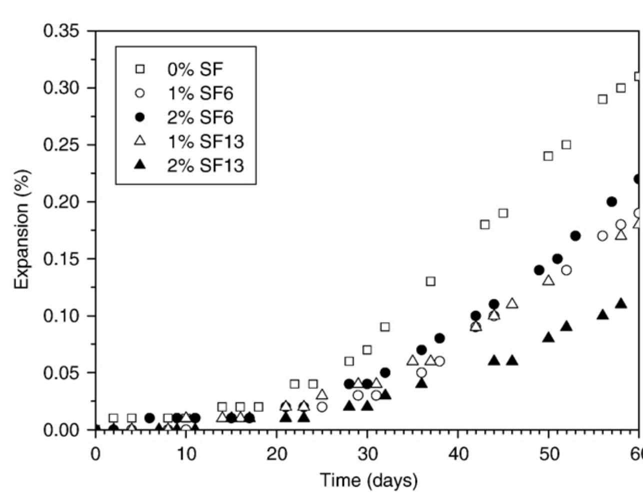

Fig. 1. Expansion by AAR.

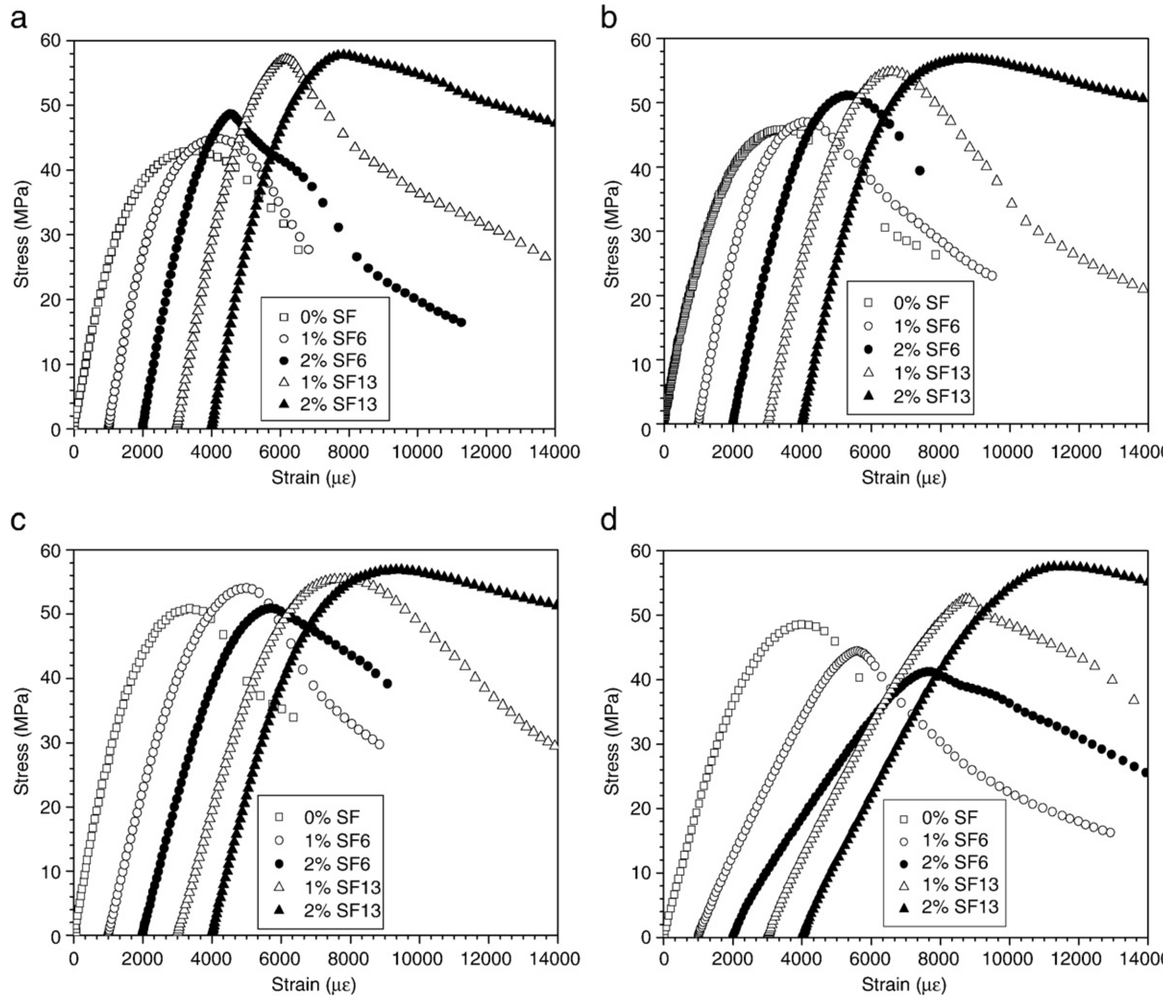

Fig. 2. Stress–strain curves for the ages: (a) 28 days; (b) 28 + 14 = 42 days; (c) 28 + 28 = 56 days; and (d) 28 + 60 = 88 days. (All curves have its origin at 0 με, they are shifted by 1 mm for better visualization).

samples were taken from the central part and also from the internal portion next to the surface of the prisms used for the AAR tests after 88 days (60 days in NaOH solution).

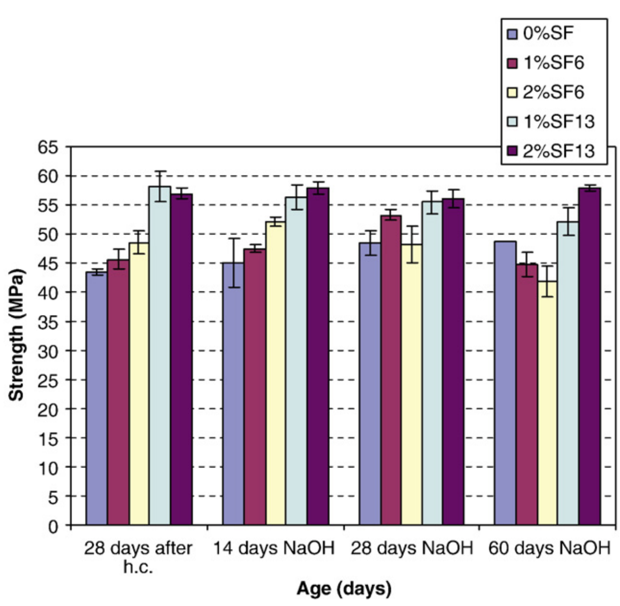

Fig. 3. Compressive strength for the several mixtures at the ages: (a) 28 days; (b) 28 + 14 = 42 days; (c) 28 + 28 = 56 days; and (d) 28 + 60 = 88 days.

3. Results and discussion

3.1. Expansion by AAR

The expansions by AAR for several mixtures described above are presented in Fig. 1. For these graphs the time zero is the time for which the bars were immersed in the NaOH 1 N solution at temperature 60 ± 2 °C. It can be noted that the addition of fibers significantly reduced the

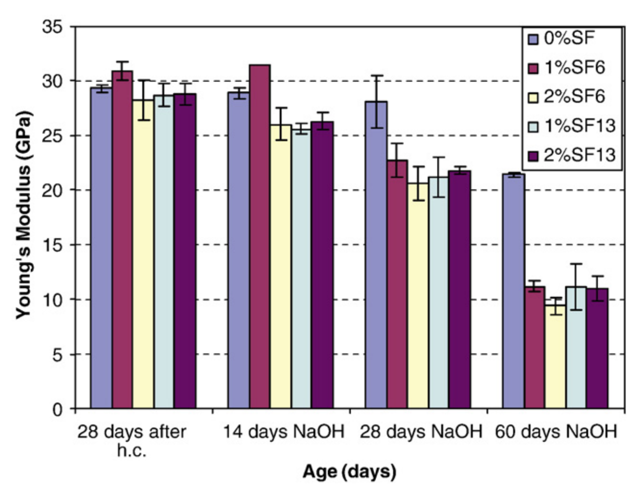

Fig. 4. Young's modulus for the several mixtures.

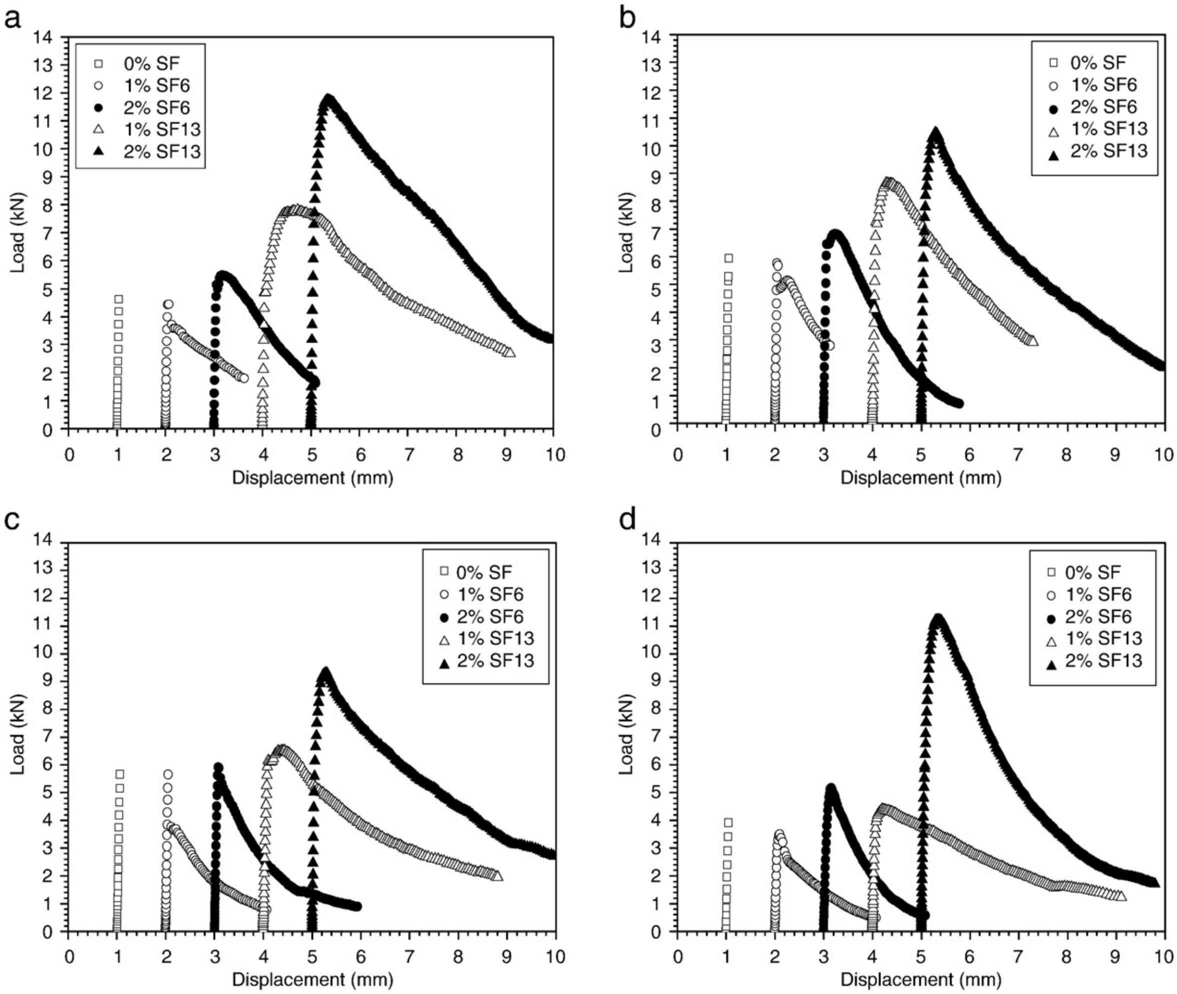

Fig. 5. Load–displacement curves in bending for the ages: (a) 28 days; (b) 28 + 14 = 42 days; (c) 28 + 28 = 56 days; and (d) 28 + 60 = 88 days. (All curves have its origin at 0 με, they are shifted by 1 mm for better visualization).

expansion by AAR. After 14 days immersed in NaOH, the mixture 0%SF showed approximately twice the expansion of the mortars containing steel fibers. After 60 days of immersion (end of the test), the mixture 2% SF13 expanded 61% less than the reference mixture. The expansions of the mixtures 1%SF6, 2%SF6 and 1%SF13 were reduced by 38%, 29% and 41%, respectively, in comparison to the 0%SF.

It may seem paradoxical that the mixtures 1%SF6 and 2%SF6 presented a similar behavior while for the fibers SF13 the benefic action of a greater fiber volume was remarkable. It is known that, besides orientation and distribution, the efficiency of the fibers for a given cementitious matrix depends on its content and aspect ratio [12]. The greater the aspect ratio the more efficient is the fiber [13]. Otherwise, increasing the content of fibers beyond a certain limit may correspond to little improvement of the mechanical properties of the composite [14]. This appears to be the case of the SF6 fibers for volume contents greater than 1%. The results reported in Section 3.2 shows that the compressive strength of 2%SF6 is lower than 1%SF6. Furthermore, the improvement verified for the flexural behavior of the mixture 2%SF6 compared to 1% SF6, is not as remarkable as the improvement verified for the composites made with the fiber SF13. In what concerns AAR expansion, it appears that, for the fiber SF6 it occurred a saturation in the control of the expansion, since the swelling of both 1%SF6 and 2% SF6 are almost similar until 45 days of exposition. In the subsequently ages, the values of expansion are slightly higher for the 2%SF6, as can be seen in Fig. 1.

3.2. Compressive strength and Young's modulus

Fig. 2 shows the stress–strain curves for all the mixtures at the ages of 28, 42, 56, and 88 days, while the graphs shown in Figs. 3 and 4 show comparative values of the compressive strength and of the Young's modulus, respectively. It could be observed that, at the age of 28 days (before immersion in the NaOH 1 N solution), the compressive strength

Table 3
Stress at first cracking in MPa and coefficient of variation (in %) indicated within parentheses.

Mixtures	Age (days)			
	28	28 + 14	28 + 28	28 + 60
0%SF	6.3 (6.6)	8.8 (1.3)	9.0 (7.2)	6.0 (2.6)
1%SF6	5.4 (2.6)	7.6 (3.4)	6.9 (8.4)	2.9 (2.8)
2%SF6	6.3 (0.2)	7.2 (7.9)	5.0 (9.4)	3.2 (3.9)
1%SF13	6.7 (6.2)	7.2 (9.4)	5.6 (3.3)	3.1 (9.4)
2%SF13	7.2 (3.6)	8.0 (4.9)	6.5 (6.1)	5.9 (17.4)

Table 4
Flexural toughness index in kN mm and coefficient of variation (in %) indicated within parentheses.

Mixtures	Age (days)			
	28	28 + 14	28 + 28	28 + 60
1%SF6	4.44 (26.48)	4.06 (25.85)	4.02 (17.81)	2.26 (17.16)
2%SF6	5.33 (13.53)	6.32 (3.02)	4.41 (13.47)	4.40 (27.68)
1%SF13	8.94 (5.62)	8.06 (13.42)	6.21 (10.38)	4.69 (17.94)
2%SF13	11.30 (11.59)	10.65 (15.41)	10.17 (9.87)	10.62 (9.06)

increased with the addition of fibers. The better performance in relation to compressive strength was obtained by mortars containing 13 mm steel fibers.

At the age of 88 days only the mixture 0%SF presented an increasing in compressive strength (12%). For the mortars 2%SF6 and 1%SF13, the compressive strength decreased by 12% and 8%, respectively. The compressive strength of the mixtures 1%SF6 and 2%SF13 did not significantly vary. To verify the effect of hydration without the action of AAR on the evolution of the compressive strength some specimens 0% SF were cured in water at 20 °C and tested at the ages of 28 days and 60 days. The increasing of the compressive strength was of 25%. A similar behavior was verified by de Larrard [15]. Hence, it can be concluded that the evolutions verified for the specimens submitted to AAR corresponded to a degradation of the material.

The Young's modulus has not changed significantly with the addition of fibers before the development of the AAR reactions (see Fig. 4, age 28 days). However, the Young's modulus decreases for all mixtures with the development of AAR reactions, indicating damage in the mortar matrix due to microcracking originated by the reactions. It seems paradoxical (with regard to the compressive strength) that the less damaged matrix is the one correspondent to the 0%SF. This phenomenon can be explained by the presence of gel in the fiber–matrix interface that reduces the friction between the rigid inclusions (fibers) and the matrix (see Section 3.4).

3.3. Bending: load–displacement curves and toughness

Fig. 5 shows the load–displacement curves in bending for all the mixtures at the ages of 28, 42, 56 and 88 days, while Table 3 shows the values of the flexural toughness index. The results shown in Fig. 5-a and Table 3 indicate that the addition of fibers did not vary significantly the stress at first cracking (σ_{cr}). Only the addition of 13.0 mm fibers increased this property. With the evolution of the AAR (Fig. 5-b, c and d) all the mixtures presented a reduction in σ_{cr}, the lower reduction corresponding to the mixture 0%SF (5%) and the higher to 1%SF13 (54%).

As expected, the tests showed that the higher the contents of fibers, the higher the capacity of the specimens to absorb energy (see Table 4). With the evolution of the reaction one can observe a reduction of up to 52% for the mixture with 1% of fibers. However, for the mixture 2%SF the reduction of *Tb* was not statistically significant.

3.4. Scanning electron microscopy

SEM/EDX analysis confirmed the presence of silico-calco-alkaline compounds for all AAR products, which presented diversified

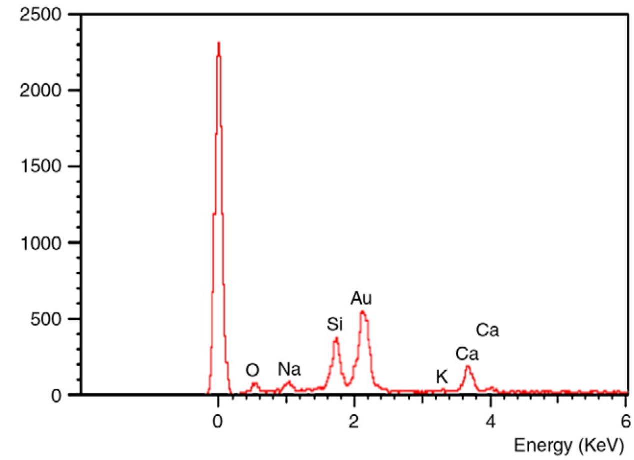

Fig. 7. EDX spectrum of the point marked in Fig. 6.

morphology. The reaction products could be detected in every sample in the following ways: filling the pores; in the interface paste/aggregate; and in the boundary of the aggregate. Silico-calco-alkaline gel was also found in the surface of the steel fibers which could have affected the mechanical properties of the interface steel-matrix. The micrographs presented in Figs. 6 to 13 show some products indentified as AAR gel as well as EDX spectra indicating the chemical composition of these compounds. A greater incidence of voids was also detected in the samples with fibers in comparison with the reference mortar, and some of them were filled with gel.

3.5. General microstructural behavior

The results presented in this paper fit with the twofold microstructural mechanism proposed by Ostertag et al. [4]. Within a microstructural approach it is accepted that the AAR gel, in a first moment, is trapped in a net of pores, voids or initial microcracks that compose the porous medium of the concrete skeleton [16]. Then, when the pores are filled, the chemomechanical coupling develops resulting in gel pressure that may induce damage in the surrounding cementitious matrix. Furthermore, as cracks grow, more space is available to the gel depositions maintaining the pressure at a constant level. A detailed formulation of this mechanism was derived by Dormieux et al. [17] within the framework of poro-micromechanics showing good agreement with experimental data.

According to the mechanism proposed by Ostertag et al. [4], the fibers bridge the cracks reducing the macroscopic mechanical

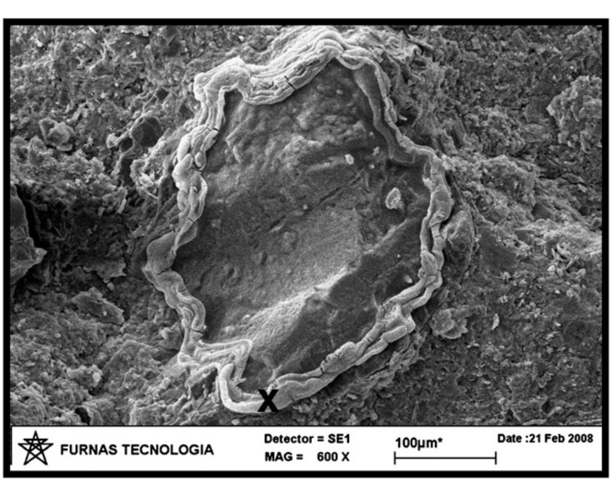

Fig. 6. 0%SF — Reactive aggregate with AAR products at its boundary.

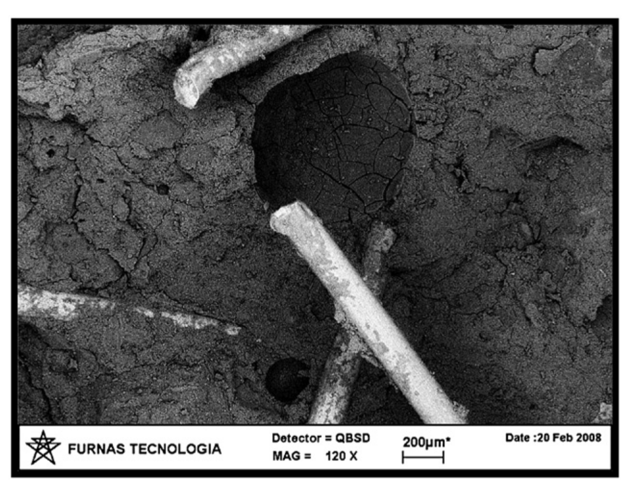

Fig. 8. 1%SF6 — Pore filled with cracked gel, and fibers around the pore.

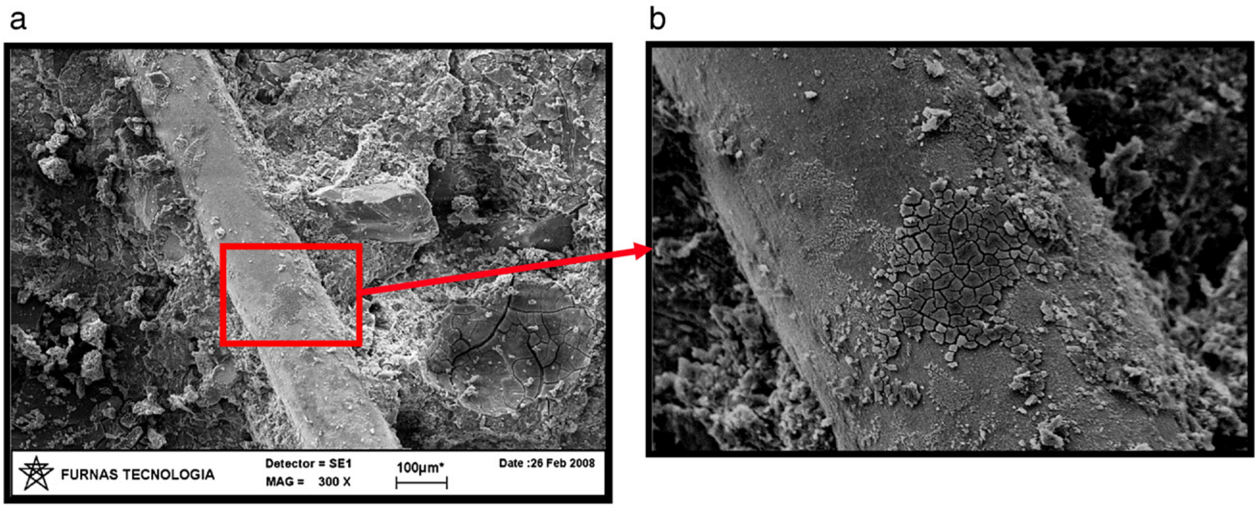

Fig. 9. 2%SF6 — Interface steel fiber/matrix (a) showing the alkali-silica gel on the surface of the fiber (b).

expansion. On the other hand, once the crack opening process is controlled by the fibers, the pressure increases and confines the gel inhibiting the development of the reaction. The former mechanism is a chemical effect provoked by the concentration of reaction products that remain close to the reaction site. In this way, the higher concentration of Si retards the dissolution of the reactive aggregate reducing the production of gel.

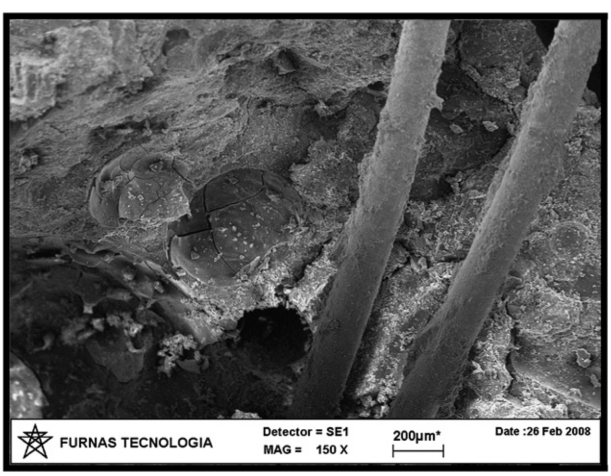

Fig. 10. 2%SF6 — Fibers close to the pores with cracked gel in its interior.

4. Concluding remarks

This paper presented a research dedicated to the study of the behavior of mortars containing steel fibers under accelerated AAR tests. For the fiber volume contents used (1% and 2%), the results indicated the beneficial action of using the fiber-reinforced material, which can significantly reduce (up to 61%) the expansion by AAR. The expansion tests were accompanied by mechanical tests which indicated the effect of the reaction on the main properties of the material. The main results of these mechanical tests indicated that even though the AAR introduces damage in the specimens, the fibers continue acting as reinforcement and do not lose their capacity to absorb energy.

The most expressive benefit corresponded to the addition of 13.0 mm fibers in the percentage of 2%. This fiber content also corresponded to the greatest increments in the mechanical properties compared to the reference mortar, mainly for the post-cracking strength and for the capacity to absorb energy in bending.

The experimental program presented in this paper indicated the potential of steel fibers to reduce the effects of alkali-aggregate reaction. However, the results are limited to a reduced set of variables,

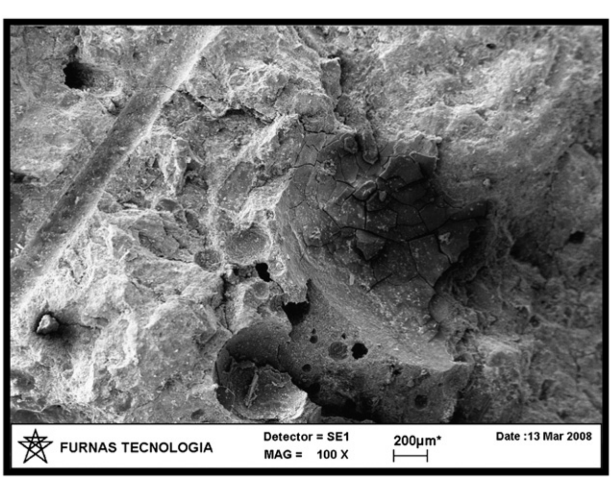

Fig. 11. 1%SF13 — Fiber groove close to a pore filled with cracked gel.

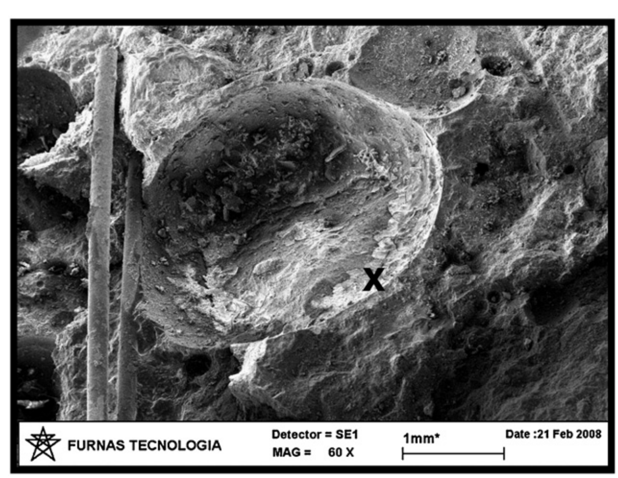

Fig. 12. 2%SF13 — Fiber close to a pore filled with AAR product, and fiber groove (at right).

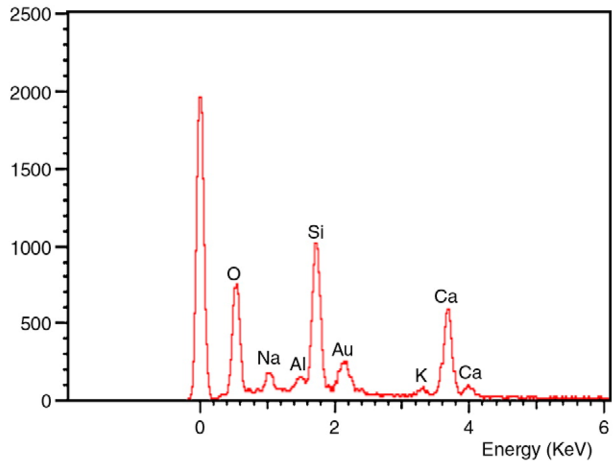

Fig. 13. Spectra taken from the point marked in Fig. 12.

and a more comprehensive research is being performed to extend the limits of the present investigation.

Acknowledgements

The authors acknowledge the financial support of the Brazilian Agency for Electrical Power (ANEEL) and the Hydropower Company of the Central Eastern Region of Brazil (FURNAS). The authors are also indebted for the support of the Brazilian Agencies CAPES and CNPq.

References

[1] E.M.R. Fairbairn, R.D. Toledo Filho, F.L.B. Ribeiro, R.C. Battista, Experimental analysis and modeling of spiral boxes reinforced with steel fibers, R&D Project reports, FURNAS and COPPE/UFRJ, 2007 in Portuguese.
[2] L. Turanli, K. Shomglin, C.P. Ostertag, P.J.M. Monteiro, Reduction in alkali-silica expansion due to steel microfibers, Cement and Concrete Research 31 (2001) 827–835.
[3] M.C. Garci Juenger, C.P. Ostertag, Effect of selective positioning of steel microfibers on alkali-silica reaction, Concrete Science and Engineering 4 (2002) 91–97.
[4] C.P. Ostertag, C. Yi, P.J.M. Monteiro, Effect of confinement on properties and characteristics of alkali-silica reaction gel, ACI Materials Journal 104 (3) (2007) 276–282.
[5] R.H. Haddad, M.M. Smadi, Role of fibers in controlling unrestrained expansion and arresting cracking in Portland cement concrete undergoing alkali-silica reaction, Cement and Concrete Research 34 (2004) 103–108.
[6] S.B. Park, B.C. Lee, Studies on expansion properties in mortar containing waste glass and fibres, Cement and Concrete Research 34 (2004) 1145–1152.
[7] ASTM, Standard test method for potential alkali reactivity of aggregates (mortar-bar method): ASTM C1260, 1997.
[8] ASTM, Standard practice for use of apparatus for the determination of length change of hardened cement paste, mortar, and concrete: ASTM C490, 2002.
[9] ASTM, Standard test method for static modulus of elasticity and Poisson ratio of concrete in compression: ASTM C469, 1987.
[10] MERCOSUR NORMA NM 55:96: Concrete — determination of bending tensile strength in prismatic specimens (in Portuguese), 1996.
[11] JCI SF4, Method of test for flexural strength and flexural toughness of fiber reinforced concrete, JCI Standards for Test Methods of Fiber Reinforced, Japan Concrete Institute, Japan, 1983, pp. 45–51.
[12] A. Bentur, S. Mindess, Fibre reinforced cementitious composites, Modern Concrete Technology Series2nd Edition, 2007.
[13] S. Yazici, G. Inan, V. Tabak, Effect of aspect ratio and volume fraction of steel fiber on the mechanical properties of SFRC, Construction and Building Materials 21 (2007) 1250–1253.
[14] P. Pierre, R. Pleau, M. Pigeon, Mechanical properties of steel microfiber reinforced cement pastes and mortars, Journal of Materials in Civil Engineering 11 (1999) 317–324.
[15] F. De Larrard, Concrete mixture proportioning: a scientific approach, Modern Concrete Technology Series, 9, E&FN SPON, London, 1999.
[16] E. Le Marchand, L. Dormieux, F.-J. Ulm, Elements of micromechanics of ASR-induced swelling in concrete structures, Concrete Science and Engineering 4 (2002) 12–22.
[17] L. Dormieux, E. Le Marchand, D. Kondo, E.M.R. Fairbairn, Elements of poro-micromechanics applied to concrete, Materials and Structures 37 (2004) 31–42.